A Programmable Laboratory Testbed in Support of Evaluation of Functional Brain Activation

R.L. Barbour[1,3], H.L. Graber[1,3], Y. Xu[1,3], Y. Pei[3], C.H. Schmitz[4], D.S. Pfeil[1], A. Tyagi[1], R. Andronica[1], D.C. Lee[2,5], S.-L. S. Barbour[3], J.D. Nichols[6], M.E. Pflieger[6]

Departments of [1]Pathology and [2]Surgery, SUNY Downstate Medical Center, Brooklyn, NY 11203 USA; [3]NIRx Medical Technologies LLC., Glen Head, NY 11545, USA; [4]NIRx Medizintechnik GmbH, Baumbachstr. 17, 13189 Berlin, FRG; [5]Department of Medicine, Interfaith Medical Center, Brooklyn, NY 11213, USA; [6]Source Signal Imaging Inc., San Diego, CA 92102

Introduction

- Near infrared spectroscopy (NIRS) and electroencephalography (EEG)
  - Complementary sensing technologies with desirable attributes:
    - Inherently compact form factor.
    - Sensitivity to hemodynamic (NIRS) and bioelectric (EEG) phenomenologies associated with neuroactivation.
  - BUT, experimental phantom-based systems, analogous to those routinely used to evaluate structural imaging methods, currently are unavailable.
    - Important for the development of functional imaging applications based on NIRS or EEG, or both in combination.
    - Used to quantitatively assess the accuracy of derived functional information.
- Addressing this, we have undertaken a technology integration effort with the following aims:
  - Ability to initiate and recover complex macroscopic behaviors that, in general, are not directly observable.
  - Implement the modeled behavior in a longitudinally stable, anthropomorphic head form that supports translation from laboratory-based to subject-based studies.
- The first aim is addressed by manufacturing programmable dynamic phantoms for hemodynamic and bioelectric behaviors.
  - Device has anthropomorphic form similar to one we reported before [1], but:
    - Important added feature is a hermitically sealed, conducting brain space that is stabilized against biological degradation.
  - Brain compartment contains programmable source elements—electrochromic cells (ECC) and electric dipoles—that can be precisely controlled electronically.
    - Manipulation of the voltage across an ECC leads changes its opacity, as a way of mimicking time-varying blood volume or oxygen saturation.
    - The dipoles can be used similarly to model time-varying EEG sources.
- The second objective is accomplished by employing the same sensing devices, headgear, and analysis resources used in human- or animal-subject studies to explore the programmable validating environment, or testbed.

Atlas-based Mapping

- Ideally, NIRS or EEG inverse-problem computations is based on knowledge of individual-subject boundary conditions.
- For cases where individualized structural information is not available, an alternative solution is to substitute a selected atlas (Fig. 3).
  - Have generated a series of overlapping regions supporting specification of arbitrary sensor arrangements.
  - A montage of standard EEG electrode locations is provided to guide assignment of NIRS optode positions.
  - Once a sensor arrangement is specified, determination of the associated imaging operators is immediately available.
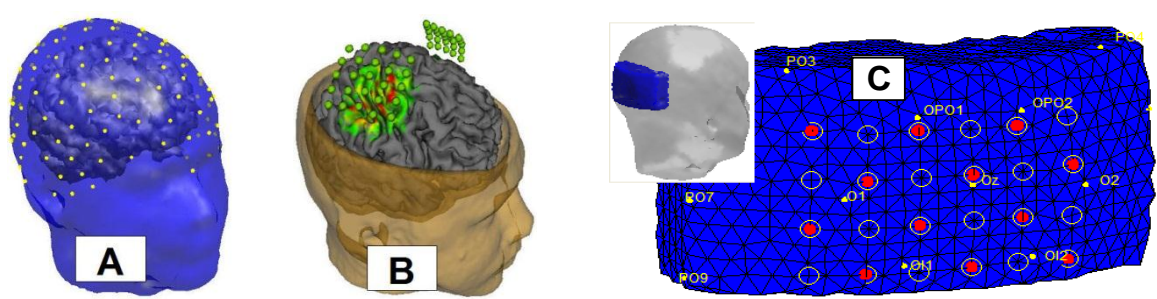

Fig. 3. Graphic summary of the developed human atlas. (A) Positions of the EEG electrodes. (B) 3D representation of NIRS optode positions and a projection of hemodynamic information onto the cortex. (C) Example of an optode sensor array placement displayed on a selected atlas segment. Open circles – detector fibers only; filled circles – co-located source and detector; yellow dots – standard EEG locations.

- Analogous process is used to generate atlases for other species, for animal-brain imaging studies.
  - Example shown here is the rhesus macaque atlas (Fig. 4).
  - Owing to the smaller head size, segmentation of the brain was not necessary.
  - Final atlas involved merging anatomical information for the head of an individual animal and a group-averaged brain structure (to minimize effects of individual variability).
- Experimental data from a macaque-head phantom, in combination with the Fig. 4 atlas, shows that the testbed provides for high spatial and temporal accuracy in recovered images (Fig. 5).

NIRS-EEG Data Analysis and Mapping Environment

- EMSE Suite (ElectroMagnetic Source Estimation, Source Signal Imaging) – software modules for integrating EEG with structural MRI [2]:
  - Spatial mapping of sensor positions and MRI co-registration.
  - Review of EEG data.
    - Spatial and temporal filters for treating artifacts.
  - Mapping signal-space measures topographically onto the head surface.
  - Computing and displaying solutions to the cortical current-density inverse-problem.
  - Display of MRI data.
    - Tissue segmentation capabilities.
  - Mesh generation based on segmented MRIs
  - Statistical nonparametric mapping.
    - In either signal space or source space.
- NAVI (Near-infrared Analysis Visualization and Imaging, NIRx Medical Technologies) [3,4] – MATLAB-based environment, includes modules for:
  - Image formation, display and analysis.
  - An electronic ledger.
    - Automatically records metadata associated with all data transformations.
  - Utilities, modeled principally after strategies supported by SPM8 [5,6]:
    - GLM-based parametric mapping of detected hemodynamic response functions.
    - Atlas-based mapping of image findings onto identified brain regions.
    - Automated anatomical labeling (AAL) functionality.
    - Examination of effective connectivity, via strategies such as dynamic causal modeling (DCM) [7].
  - Flowchart (Fig. 6) depicts the logical structure of the integrated analysis environment.

Testbed Components

Anthropomorphic Dynamic Phantom

- The approach of [1] has been extended by introducing a "brain" into the phantom [Fig. 1(A)].
  - Made of hydrogel-based biopolymer with saline added to mimic impedances typical of real tissue.
  - Commonly available stabilizers are included to inhibit bacterial and mold growth.
  - TiO_2 and India Ink are added to provide physiologically plausible optical coefficients.
- Embedded source array includes two different types of signal-generating arrangements [Fig. 1(B)].
  - An ECC, dipole and locating light-emitting diode (LED).
    - Supports modeling of induced neural signals and accompanying local hemodynamic responses.
    - All are within an integrated assembly with linear dimensions of ~1.5 cm.
  - Deeper-lying dipoles.
    - Model bioelectric sources that are detectable by EEG but not by NIRS measurements.
- By varying the voltage across an ECC, user can generate opacity-vs-time functions that mimic hemodynamic responses of interest (Fig. 2).
- Electronic elements independently controllable.
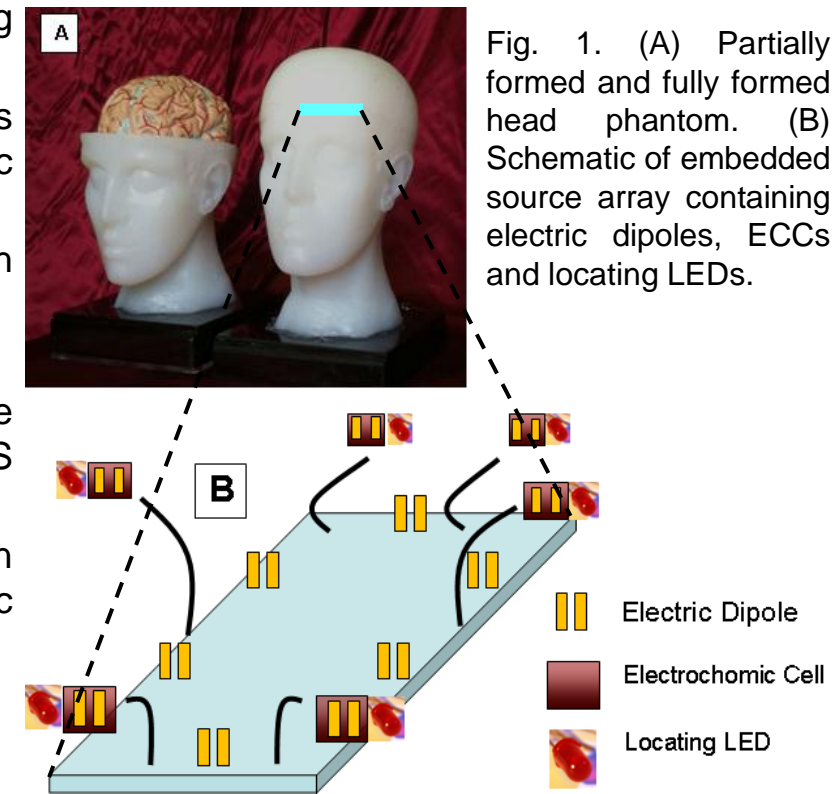
Fig. 1. (A) Partially formed and fully formed head phantom. (B) Schematic of embedded source array containing electric dipoles, ECCs and locating LEDs.
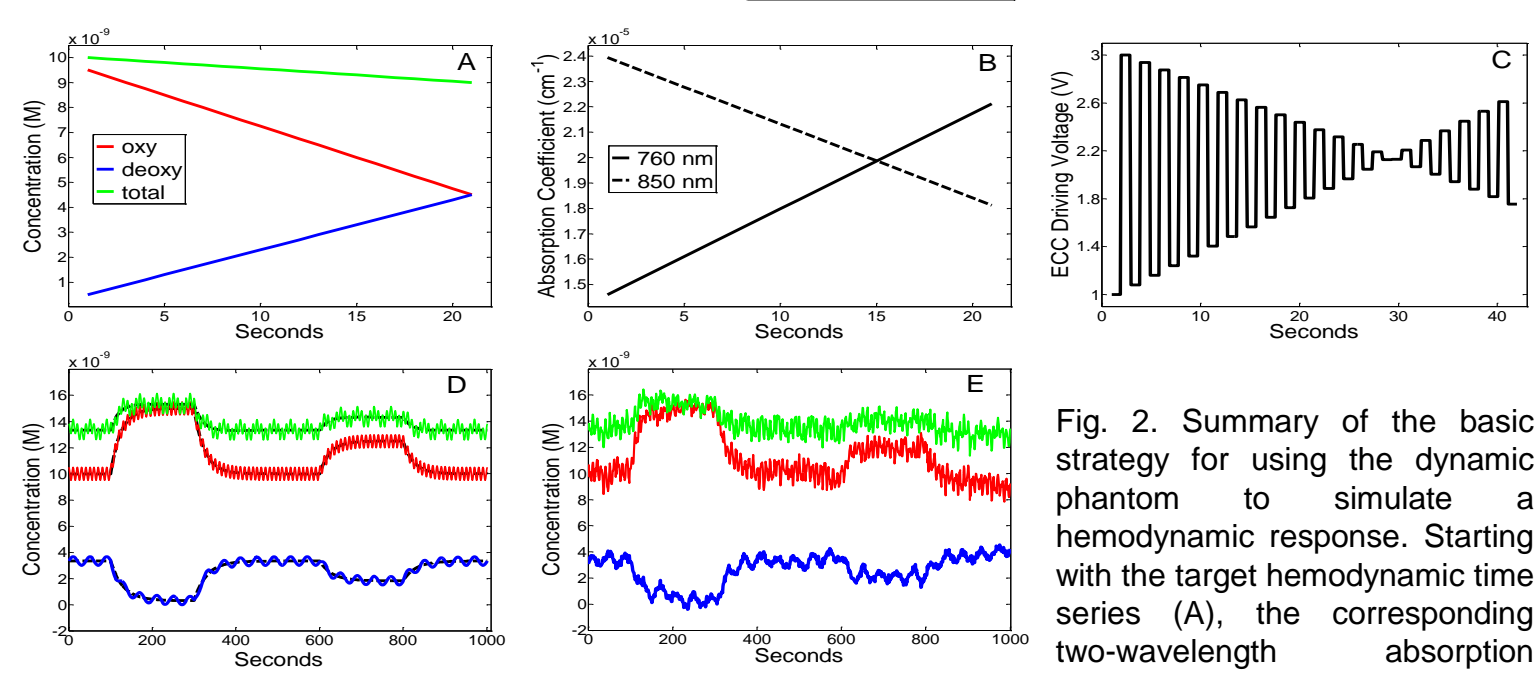
Fig. 2. Summary of the basic strategy for using the dynamic phantom to simulate a hemodynamic response. Starting with the target hemodynamic time series (A), the corresponding two-wavelength absorption coefficients are computed (B), and then the appropriate voltage-vs.-time sequence for driving the ECCs (C). (D) An idealized example of task-related hemodynamic responses, with physiological oscillations overlaid. (E) the recovered hemodynamic responses computed from experimental phantom data. Color coding in Panels D and E is the same as that in Panel A.
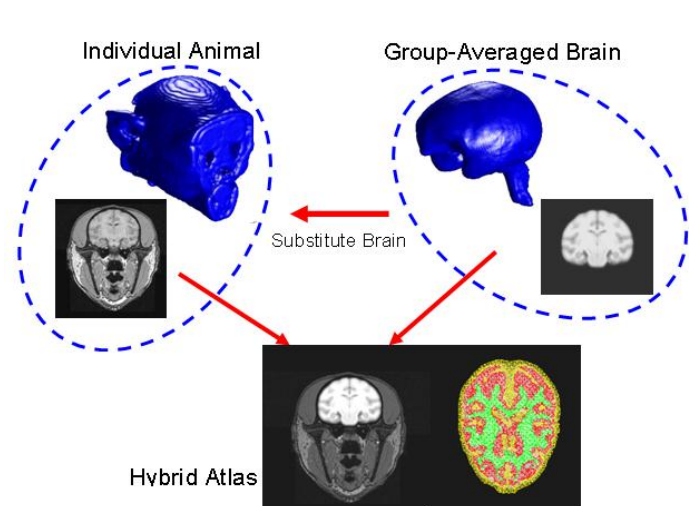
Fig. 4. Schematic of the process used to create the macaque atlas. Information from a group-averaged brain is superimposed onto an individual MRI scan to yield the hybrid atlas. Bottom right image shows one of the segmented and tessellated slices from the atlas.
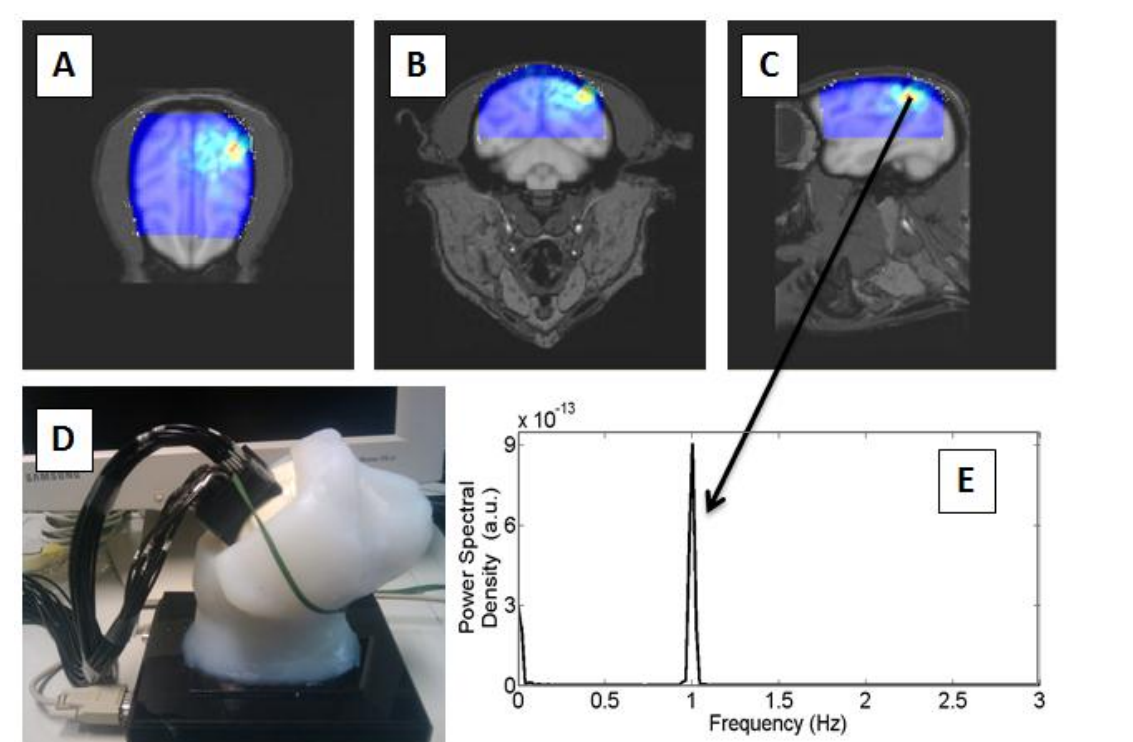
Fig. 5. Sample macaque phantom study. (D) shows a photograph of the phantom with fibers attached. (A)-(C) show horizontal, coronal, and sagittal views of the reconstructed image, highlighting the location of the ECC. (E) shows that after computing the PSD of the image time series, the 1-Hz sinusoidal driving function was recovered.

Fig 6. Flowchart for integrated NIRS/EEG framework. The common anatomical framework is provided by structural MRI.

Demonstrational Application

- The time-varying voltage signals shown in Fig. 7 were used to drive three ECCs of a phantom similar to the one in Fig. 1(A).
  - The ECCs are embedded in locations corresponding to the right frontal ('A'), temporal ('B') and occipital ('C') cortices.
  - The driving functions were derived by numerically solving a mathematical model [7] for the net hemodynamic response (blood volume, in this example) of cortical regions that interact with each other in an effective connectivity network (Fig. 8, Network 1):
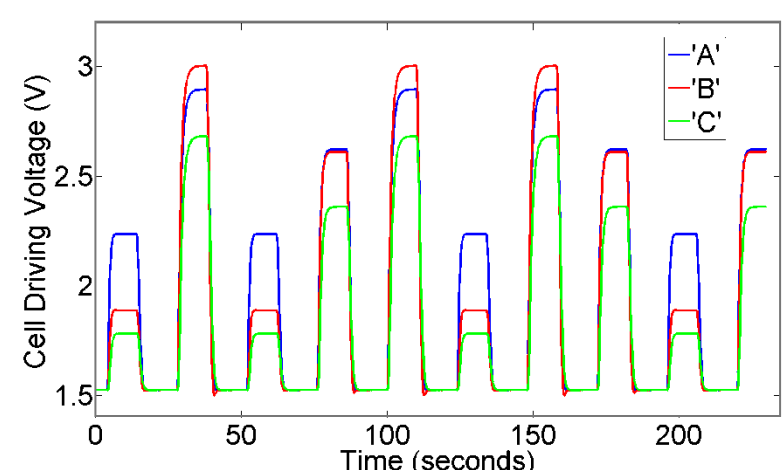

Fig 7. Time courses of the driving voltages delivered to the ECCs. The plotted functions model hemodynamic responses of cortical regions effectively connected as sketched in Fig. 8.
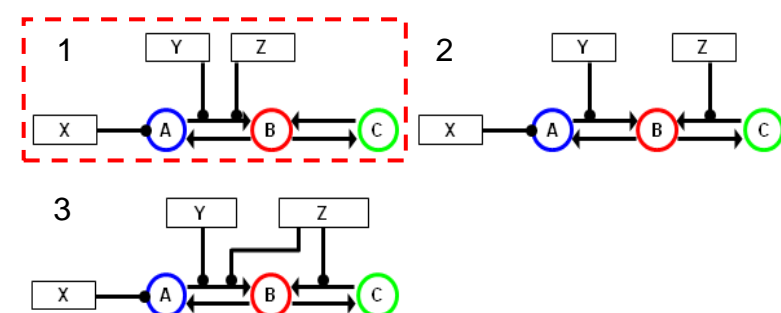

Fig. 8. The three effective connectivity networks that are supplied as inputs to the DCM inverse problem code, as plausible hypotheses for the connectivity present in the testbed model. For the phantom experiment, Network 1 (red dotted border) is correct.

- A large-area sensing array and headgear developed for human-subject studies (NIRx Medical Technologies) were used to collect steady-state NIRS time-series data.
- Data pre-processing and image reconstruction were performed using NAVI and the three human-head atlas segments corresponding to the selected head regions.
- With the driving-voltage time series as model functions (Fig. 9), the NAVI GLM image analysis utility was used to identify image pixels whose reconstructed absorption coefficient time series are significantly accounted for by the models.
  - The resulting image volumes were interpolated onto the brain-atlas cortical surface (Fig. 10), using NAVI utilities developed for identification of activated regions.
  - Volume-averaged image time series from the colored regions in Fig. 10 were used as input for DCM model-selection computations.
    - The correct model's log-evidence value is larger than the two alternative hypotheses by either 103(2) or 89.4(3) units.
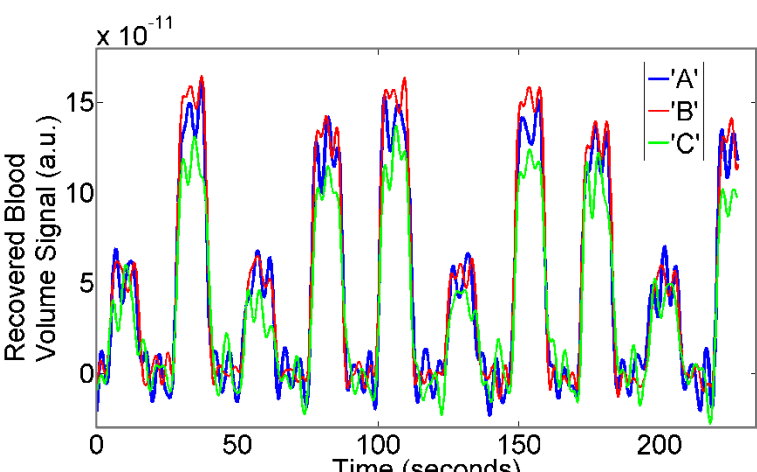
- In a follow-up experiment, 0.1-Hz sinusoidal waves were added to the Fig. 7 driving functions, as a model of background physiological rhythms (e.g., vasomotion).
  - Temporal and spatial accuracy comparable to Figs. 9 and 10 results still is achieved.
  - If the image data are not filtered to minimize the background contribution, the computed log-evidence values indicate that the incorrect network structures are preferred to the correct one, by 19.8(2) or 25.4(3) units.
  - After bandpass filtering, the correct connectivity (Network 1) is again preferred, by 39.5 units for Network 2 and by 5.2 units for Network 3.

Conclusions

Here we have described elements of a new experimental testbed that is intended to support evaluation of the principal observable elements of neural activity using hemodynamic and bioelectric sensing methods. The developed fabrication techniques are easily adopted to support generation of anatomically accurate forms that are longitudinally stable and contain embedded sources that are freely programmable. When operated together with the developed analysis environment, the configured system is intended to meet various practical needs as well as modeling of complex macroscopic neural phenomenologies.

Fig 9. Spatial mean blood-volume time series, over all image pixels that have a statistically significant (p < 1e-6) GLM fit to the corresponding driving function (Fig. 7).
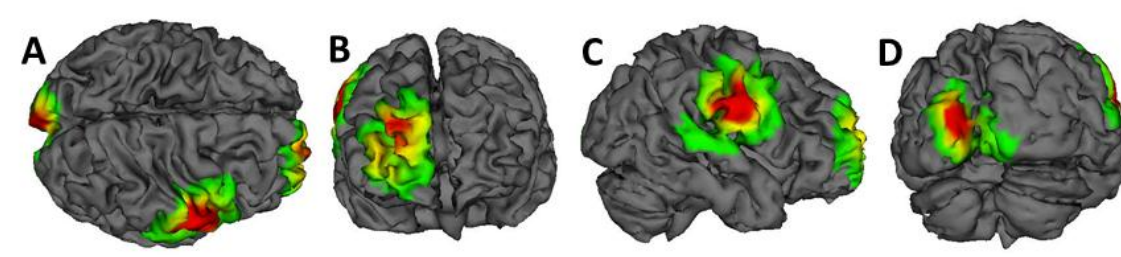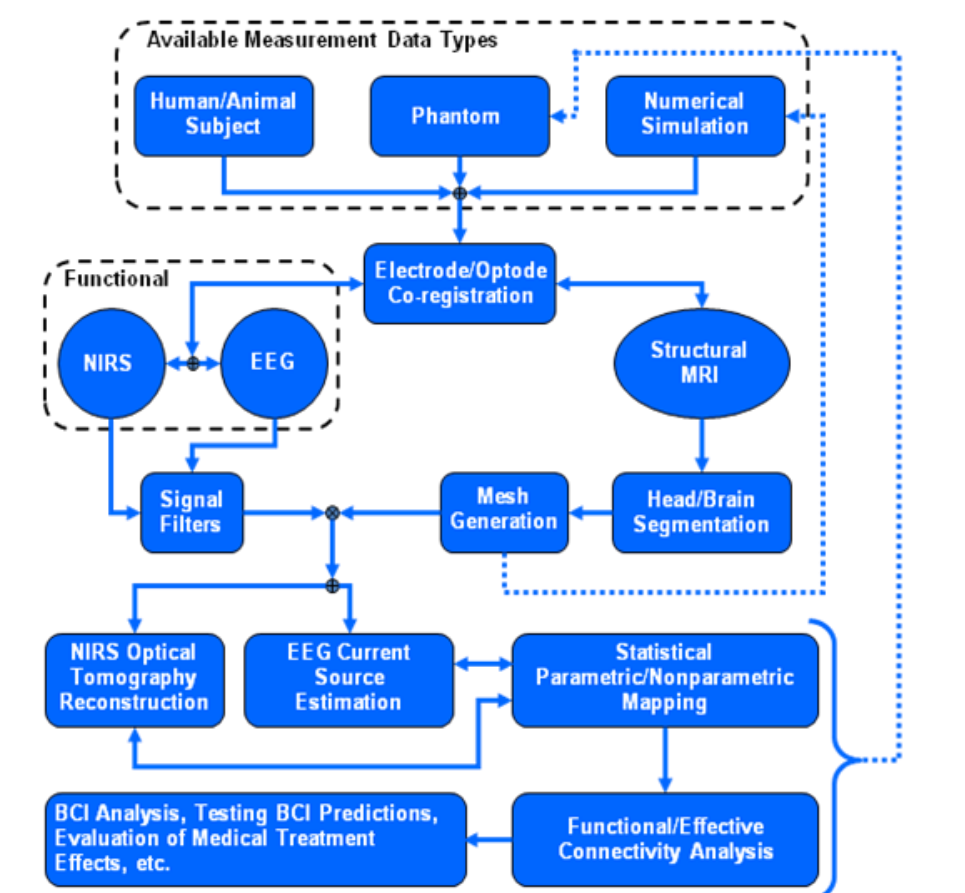

Fig 10. Cortical surface mapping of GLM coefficients. Plotted quantity (arbitrary units) is the value of the GLM β parameter obtained by fitting the appropriate ECC driving function to the tissue blood volume time series in each image pixel. A – top view, B – frontal view, C – right-lateral view, D – occipital view.

[1] R. L. Barbour, R. Ansari, R. Al abdi, H. L. Graber, M. B. Levin, Y. Pei, C. H. Schmitz, and Y. Xu, "Validation of near infrared spectroscopic (NIRS) imaging using programmable phantoms," Paper 687002 in Design and Performance Validation of Phantoms Used in Conjunction with Optical Measurements of Tissue (Proceedings of SPIE, Vol. 6870), R.J. Nordstrom, Ed. (2008).

[2] Source Signal Imaging, Inc., EMSE®Suite User Manual, Version 5.4, San Diego, 2011. Available at: ftp://ftp.sourcesignal.com/manuals/

[3] Y. Pei, Z. Wang, and R.L. Barbour, "NAVI: A problem solving environment (PSE) for NIRS data analysis," Poster No. 685 T-AM at Human Brain Mapping 2006 (Florence, Italy, June 11-15, 2006).

[4] NIRx NIRS Analysis Environment User's guide. Available at: http://otg.downstate.edu/Publication/NIRxPackage_02.pdf.

[5] W. D. Penny, K. J. Friston, J. T. Ashburner, S. J. Kiebel, and T. E. Nichols, Statistical Parametric Mapping: The Analysis of Functional Brain Images. Academic Press, 2006.

[6] N. Tzourio-Mazoyer, B. Landeau, D. Papathanassiou, F. Crivello, O. Etard, N. Delcroix, B. Mazoyer, and M. Joliot, "Automated anatomical labeling of activations in SPM using a macroscopic anatomical parcellation of the MNI MRI single-subject brain," NeuroImage 15, 273-289 (2002).

[7] K. Friston, "Causal modeling and brain connectivity in functional magnetic resonance imaging," PLoS Biology 7, 0220-0225 (2009).